Communications in Physics, Vol. 33, No. 4 (2023), pp. 399-410
DOI: https://doi.org/10.15625/0868-3166/18214

Double electromagnetically induced transparency in a four-level lambda atomic system with Doppler broadening

Nguyen Huy Bang[1], **Le Van Doai**[1], **Hoang Minh Dong**[2] and **Nguyen Thi Thu Hien**[2,†]

[1]*Vinh University, 182 Le Duan Street, Vinh City, Vietnam*
[2]*Ho Chi Minh City University of Industry and Trade, Ho Chi Minh City, Vietnam*

E-mail: [†]hien0ntt@gmail.com

Received 2 April 2023; *Accepted for publication 4 August 2023*; *Published 4 December 2023*

Abstract. *In this paper, we study the formation of two electromagnetically induced transparency (EIT) windows in a four-level lambda atomic system with Doppler broadening. The depth and the width of the EIT windows are easily changed by adjusting the intensity of the controlling laser fields. Meanwhile, the position of the EIT windows is also easily shifted by changing the frequency of the laser fields. In particular, by turning on or off one of the two coupling laser fields, the probe field response can be switched between one or two EIT window regimes, i.e., it is possible to switch between absorption and transparency regimes, and vice versa. In addition, our analytical model also allows one to investigate the influence of temperature (or Doppler width) on EIT windows, which is necessary for experimental observations as well as related applications at room temperature.*

Keywords: effects of atomic coherence.
Classification numbers: 42.50.Gy; 42.65.-k.

1. Introduction

Even though electromagnetically induced transparency (EIT) has been well-studied over the last few decades [1, 2], physicists and scientists still express their keen interest in both theoretical and experimental studies with different excited atomic configurations [3–6]. These excitements may result from the various application ranges of EIT materials in the fields of quantum computer and modern photonic devices [7]. The earliest models of EIT were proposed for three-level atomic systems which resulted only in one EIT window [8, 9]. As for our present time frame, the current EIT studies are focusing on four-level atomic systems with two EIT windows [10–14] and five-level atomic systems with three EIT windows [15, 16], and so on. The advantage of multi-EIT materials is the ability to create multi-channel operations in applied devices, enabling them to

switch between absorption regime and transparency regime easily. This feature also enables the formation of various desired optical nonlinear effects. However, there are obstacles to creating multi-window EIT such as simultaneous adjustment of laser fields and reduction in transparency efficiency. Therefore, double EIT models are often perceived to be superior.

At present, several double EIT models for four-level atomic systems have been proposed, for example, four-level N-type [10], inverted Y- type [11], Y-type [14], tripod-type [7, 12, 17, 18] configurations. In addition to theoretical studies, several experimental studies on EIT in four-level systems have also been published [10, 19]. Recently, multi-level EIT systems have found various applications such as optical bistability [12], optical switching [7], slow light [14], Kerr nonlinearity [19], and so on. Among all models of EIT in the four-level systems, the lambda configuration is more interesting than others because it is easy to create double window EIT with high transparency efficiency and therefore it is easy to observe experimentally. Yet, still there have been no studies on EIT in the four-level lambda configuration with Doppler broadening. Such an EIT model is essential for experimental studies and relevant applications at room temperature. Additionally, we proposed a success in the development of the analytical EIT model for a five-level ladder-type atomic system with Doppler broadening, and this model was successful in our experimental observations of multiple EIT windows at room temperature [15, 16]. However, the model only uses one coupling laser field for the generation of three-window EIT, so it is also difficult to control the EIT windows independently.

In this paper, we develop an analytical model of EIT in a four-level lambda-type atomic system under the presence of Doppler effect. The model uses two coupling laser fields for generating two EITs independently. The absorption and dispersion coefficients of the system with Doppler broadening are obtained. The influences of the intensity and frequency detuning of the controlling laser fields, as well as temperature of the atomic medium on the EIT formation are considered.

2. Theoretical model and basic equations

The semi-classical theory, which means the laser fields are treated according to classical theory while the atoms are treated in accordance with quantum mechanics, is used to describe the interaction between the laser fields and the atoms [20]. In this model, three laser fields with different frequencies are applied to the atomic system as follows: one weak probe laser field is specified with frequency ω_p and Rabi frequency ω_p to excite the transition $|1rangle \leftrightarrow |4\rangle$, while two strong controlling laser fields are respectively named as the coupling laser field with frequency ω_c and Rabi frequency ω_c to excite the transition $|2\rangle \leftrightarrow |4\rangle$ and the signal laser field with frequency ω_s and Rabi frequency ω_s to excite the transition $|3\rangle \leftrightarrow |4\rangle$. Energy levels of this four-level atom are described in Fig. 1. Let Δ_p, Δ_c , and Δ_s be frequency detunings of probe field, coupling field, and signal field compared with the transition frequency from levels $|1\rangle$, $|2\rangle$ and $|3\rangle$ to level $|4\rangle$ with their definitions as $\Delta_p = \omega_{41} - \omega_p$, $\Delta_c = \omega_{42} - \omega_c$ and $\Delta_s = \omega_{43} - \omega_s$, with ω_{41} , ω_{42} and ω_{43} are the angular frequency differences between level $|4\rangle$ and levels $|1\rangle$, $|2\rangle$ and $|3\rangle$, respectively.

Assume that the strong controlling laser fields only cause precise transitions of designated states and they do not affect any further levels. The total Hamiltonian of the system includes the Hamiltonian of the free atom H_0 and the interaction Hamiltonians of the light fields with the atom V_p , V_c and V_s [20]:

$$H = H_0 + V_p + V_c + V_s, \tag{1}$$

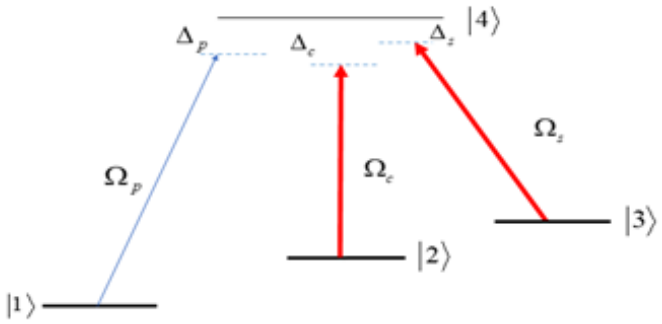

Fig. 1. Diagram of four-level lambda-type atomic system.

where, in the electric dipole approximation,

$$H_0 = \sum_{m=1}^{4} \hbar\omega_m |m\rangle \langle m|, \tag{2}$$

with ω_m (m = 1, 2, 3, 4) is the angular frequency of level $|m\rangle$ and

$$V_p = \frac{\hbar\Omega_p}{2}\left(|1\rangle\langle 4| e^{-i\omega_p t} + |4\rangle\langle 1| e^{i\omega_p t}\right), \tag{3}$$

$$V_c = \frac{\hbar\Omega_c}{2}\left(|2\rangle\langle 4| e^{-i\omega_c t} + |4\rangle\langle 2| e^{i\omega_c t}\right), \tag{4}$$

$$V_s = \frac{\hbar\Omega_s}{2}\left(|3\rangle\langle 4| e^{-i\omega_s t} + |4\rangle\langle 3| e^{i\omega_s t}\right). \tag{5}$$

The density matrix method is also used to determine the atomic states through density matrix ρ with and is the atomic system wave function. The Schrodinger equation is then substituted by the Liouville equation [20]:

$$\frac{\partial\rho}{\partial t} = -\frac{i}{\hbar}[H,\rho] - (\gamma\rho), \tag{6}$$

where $(\gamma\rho)$ describes the relaxation processes in the atomic system. From Eqs. (2)-(6) and using the rotating wave approximation, the matrix elements of the four-level system are written as:

$$\dot{\rho}_{11} = \left(\frac{i\Omega_p}{2}\right)(\rho_{14} - \rho_{41}) + \Gamma_{14}\rho_{44} \tag{7}$$

$$\dot{\rho}_{22} = \left(\frac{i\Omega_c}{2}\right)(\rho_{24} - \rho_{42}) + \Gamma_{24}\rho_{44} \tag{8}$$

$$\dot{\rho}_{33} = \left(\frac{i\Omega_s}{2}\right)(\rho_{34} - \rho_{43}) + \Gamma_{34}\rho_{44} \tag{9}$$

$$\dot{\rho}_{44} = \left(\frac{i\Omega_p}{2}\right)(\rho_{41} - \rho_{14}) + \left(\frac{i\Omega_c}{2}\right)(\rho_{42} - \rho_{24}) + \left(\frac{i\Omega_s}{2}\right)(\rho_{43} - \rho_{34}) - (\Gamma_{14} + \Gamma_{24} + \Gamma_{34})\rho_{44} \tag{10}$$

$$\dot{\rho}_{12} = i\rho_{12}(\Delta_p - \Delta_c) + \left(\frac{i\Omega_c}{2}\right)\rho_{14} - \left(\frac{i\Omega_p}{2}\right)\rho_{42} - \gamma_{21}\rho_{12} \tag{11}$$

$$\dot{\rho}_{13} = i\rho_{13}(\Delta_p - \Delta_s) + \left(\frac{i\Omega_s}{2}\right)\rho_{14} - \left(\frac{i\Omega_p}{2}\right)\rho_{43} - \gamma_{31}\rho_{13} \tag{12}$$

$$\dot{\rho}_{14} = i\rho_{14}\Delta_p + \left(\frac{i\Omega_p}{2}\right)(\rho_{11} - \rho_{44}) + \left(\frac{i\Omega_c}{2}\right)\rho_{12} + \left(\frac{i\Omega_s}{2}\right)\rho_{13} - \gamma_{41}\rho_{14} \tag{13}$$

$$\dot{\rho}_{23} = i\rho_{23}(\Delta_c - \Delta_s) + \left(\frac{i\Omega_s}{2}\right)\rho_{24} - \left(\frac{i\Omega_c}{2}\right)\rho_{43} - \gamma_{32}\rho_{23} \tag{14}$$

$$\dot{\rho}_{24} = i\rho_{24}\Delta_c + \left(\frac{i\Omega_c}{2}\right)(\rho_{22} - \rho_{44}) + \left(\frac{i\Omega_p}{2}\right)\rho_{21} + \left(\frac{i\Omega_s}{2}\right)\rho_{23} - \gamma_{42}\rho_{24} \tag{15}$$

$$\dot{\rho}_{34} = i\rho_{34}\Delta_s + \left(\frac{i\Omega_s}{2}\right)(\rho_{33} - \rho_{44}) + \left(\frac{i\Omega_p}{2}\right)\rho_{31} + \left(\frac{i\Omega_c}{2}\right)\rho_{32} - \gamma_{43}\rho_{34} \tag{16}$$

where Γ_{mn} is the rate of spontaneous population decay from the level $|m\rangle$ to the level $|n\rangle$, and Γ_{mn} is defined as the rate of the atomic coherence decay between the level $|m\rangle$ and the level $|n\rangle$. The elements describing population are interrelated through normalized condition:

$$\rho_{11} + \rho_{22} + \rho_{33} + \rho_{44} = 1. \tag{17}$$

In order to investigate the absorption and dispersion properties of the atomic medium for the probe field, we find the solution of the density matrix element ρ_{41} in the stationary state. Assume that the atom is initially in the ground state, i.e., and . Therefore, from equations (11)-(13) we get the solution ρ_{41} as follows:

$$\rho_{41} = \frac{\frac{i\Omega_p}{2}}{\gamma_{41} - i\Delta_p + \frac{\frac{\Omega_c^2}{4}}{\gamma_{21} - i(\Delta_p - \Delta_c)} + \frac{\frac{\Omega_s^2}{4}}{\gamma_{31} - i(\Delta_p - \Delta_s)}}. \tag{18}$$

The density matrix element is related to the susceptibility of the atomic medium through the equation:

$$\chi = \frac{2Nd_{41}^2}{\varepsilon_0 \hbar \Omega_p}\rho_{41}, \tag{19}$$

where ε_0 is the vacuum permittivity, N is the atomic density of the sample and d_{41} is the electric-dipole matrix element between the levels $|1\rangle$ and $|4\rangle$.

In further study on Doppler broadening effect, we assume that the controlling laser fields and the probe laser field have a similar propagation direction as the atoms moving at velocity v. Because of Doppler transition, frequency detunings of the laser fields can be re-written as ; and . In this case, the number of particles moving at velocity v parallel to the laser fields is calculated by Maxwell-Boltzmann distribution at thermal equilibrium:

$$dN(v) = \frac{N}{u\sqrt{\pi}}e^{-v^2/u^2}dv, \tag{20}$$

where $u = \sqrt{\frac{3k_BT}{m}}$ is the root mean square velocity of the atoms. Therefore, the susceptibility, Eq. (19), is rewritten as:

$$\chi(v)dv = \frac{2Nd_{41}^2}{\varepsilon_0\hbar u\sqrt{\pi}}\frac{e^{-v^2/u^2}}{z(v)}dv \tag{21}$$

with $z(v) = \gamma_{41} - i\left(\Delta_p - \frac{v}{c}\omega_p\right) + \frac{\Omega_c^2/4}{\gamma_{21}-i(\Delta_p-\Delta_c)+i\frac{v}{c}(\omega_p-\omega_c)} + \frac{\Omega_s^2/4}{\gamma_{31}-i(\Delta_p-\Delta_s)+i\frac{v}{c}(\omega_p-\omega_s)}$. Finally, the susceptibility with Doppler broadening is obtained by integrating the expression (21) over the velocity v from $-\infty$ to $+\infty$ as:

$$\chi = \frac{i\sqrt{\pi}Nd_{41}^2}{\hbar\varepsilon_0(\omega_p u/c)}e^{z^2}\left[1 - erf(z)\right] \tag{22}$$

with $z = \frac{c}{\omega_p u}\left(\gamma_{41} - i\Delta_p + \frac{\Omega_c^2/4}{\gamma_{21}-i(\Delta_p-\Delta_c)} + \frac{\Omega_s^2/4}{\gamma_{31}-i(\Delta_p-\Delta_s)}\right)$ and $erf(z)$ is the error function, which is determined by $erf(z) = \frac{2}{\sqrt{\pi}}\int_0^z e^{-t^2}dt$.

On the other hand, the real part χ' and the imaginary part χ'' of the susceptibility are respectively proportional to refraction index (n) and absorption coefficient (α) of the medium through the following formulas:

$$\alpha = \frac{\omega_p n_0 \chi''}{c}, \tag{23}$$

$$n = \frac{\omega_p n_0 \chi'}{2c}. \tag{24}$$

with n_0 being the background refractive index.

3. Results and discussion

In this section, the Rb^{87} atom [21] is used to simulate in the variant states, as follows: $|1\rangle = 5S_{1/2}, F = 1, m_F = 1$; $|2\rangle = 5S_{1/2}, F = 1, m_F = 0$; $|3\rangle = 5S_{1/2}, F = 1, m_F = -1$ and $|4\rangle = 5P_{3/2}, F = 2, m_F = 0$. Here, F denotes the quantum number of total angular moment at the investigating state. The atomic spontaneous emission rates are $\Gamma_{21} = \Gamma_{31} = 0.03$ MHz and $\Gamma_{41} = 3$ MHz.

3.1. Controlling the position of the EIT windows

First, we investigate the influence of the frequency detuning of the controlling laser fields on the formation of EIT windows. In this case, the intensity of the controlling laser fields is unchanged as ω_c = ω_s =150 MHz and it is assumed that the atomic medium is observed at room temperature T = 300 K. Afterwards, we plot the graph of absorption (solid line) and dispersion (dashed line) versus the frequency detuning of the probe field at different values of frequency detuning of the controlling fields: (a) Δ_c = Δ_s = 0, (b) Δ_c = Δ_s = -100 MHz, (c) Δ_c = Δ_s = 100 MHz, (d) Δ_c = 0 and Δ_s = 100 MHz, (e) Δ_c = 0 and Δ_s = -100 MHz, (f) Δ_c = 100 MHz and Δ_s = -100 MHz. As is known that, the occurrence of the EIT windows is the result of the quantum interference among the transitions from the levels $|1\rangle$, $|2\rangle$ and $|3\rangle$ to the level $|4\rangle$ which is created by weak probe laser field and strong controlling laser fields, so that we obtain 2 EIT windows as depicted in Fig. 2. In Fig. 2(a), when $\Delta_c = \Delta_s = 0$ the two EIT windows overlap, so we only see one EIT window at the position Δ_p = 0. The appearance of the EIT window satisfies the two-photon resonance condition on the frequency of the probe and controlling laser fields. Specifically, the EIT window is induced by the coupling field, the two-photon resonance condition Δ_c - Δ_p = 0, and

the EIT window is induced by the signal field as Δ_c - Δ_p = 0. Therefore, when $\Delta_c = \Delta_s = 0$, the EIT windows induced by the coupling and signal fields are located at position $\Delta_p = 0$. The phenomenon and its explanation are similar in Figs. 2(b) and 2(c) when Δ_c is equal to Δ_s. However, the position

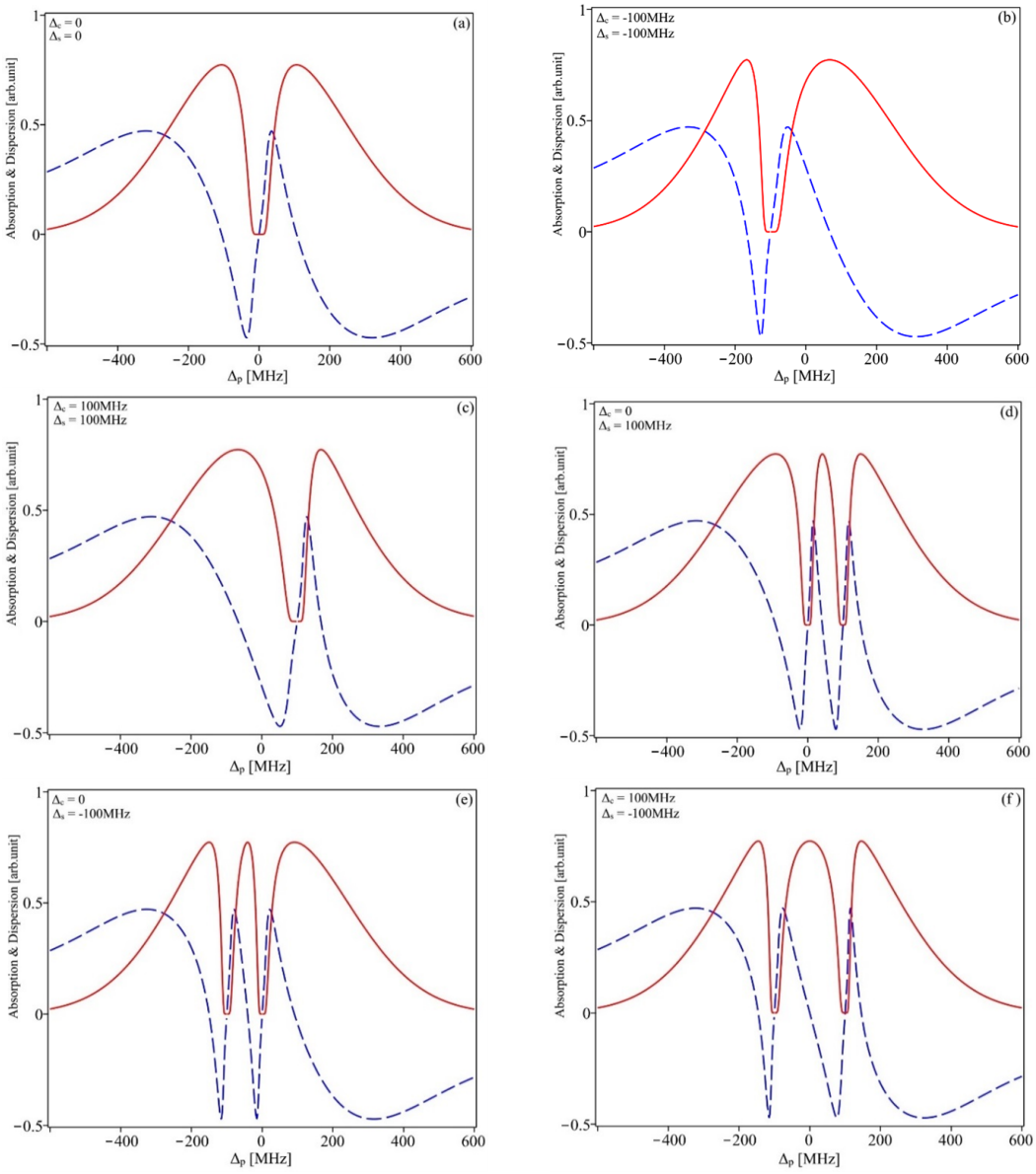

Fig. 2. Absorption and dispersion graphs with respect to frequency detuning of the probe laser field at different values of coupling and signal detunings. In the figures, the solid lines represent absorption and the dashed lines represent dispersion. The graphs are constructed at a constant temperature 300 K. Other parameters remain unchanged: $\omega_c = \omega_s$ =150 MHz and ω_p = 0.05 MHz.

of this dual EIT window can be shifted left or right on the Δ_p-axis. For example, in Fig. 2(b) with $\Delta_c = \Delta_s$ = -100 MHz, this EIT window is located at position Δ_p = -100 MHz, while when $\Delta_c = \Delta_s$ = 100 MHz, it is located at position Δ_p = 100 MHz (Fig. 2(c)). These results indicate a similar role of the two controlling laser fields in creating EIT windows in this four-level lambda-type atomic medium. In other cases where $\Delta_c \neq \Delta_s$, the two EIT windows are separated. Indeed, when Δ_c = 0 and Δ_s = 100 MHz, the first EIT window occurs at the position Δ_p = 0 caused by the coupling laser field, while the second occurs at the position Δ_p = 100 MHz caused by the signal laser field, as shown in Fig. 2(d). On the other hand, when Δ_c = 0 and Δ_s = -100 MHz in Fig. 2(e), the second one in Fig. 2(d) is shifted to the left and located in the position Δ_p = -100 MHz. When Δ_c = 100 MHz and Δ_s = -100 MHz, two EIT windows are observed to be symmetric through the resonance position Δ_p = 0, as in Fig. 2(f). Especially, in this case (Fig. 2(f)) we can see that a transparency spectral region can be converted to an absorption spectral region and vice versa by adjusting the frequency detuning of the coupling laser field and/or the signal laser field. This valuable property is considerably significant in controlling light propagation characteristics in an atomic medium. Furthermore, the change in the position of the EIT windows also leads to the shift in the dispersion curves. In particular, when $\Delta_s = \Delta_c$ = 0 (Fig. 2(a)), two normal dispersion curves overlap at the position Δ_p = 0. Likewise, when $\Delta_c = \Delta_s$ = -100 MHz (Fig. 2(b)) or $\Delta_c = \Delta_s$ = 100 MHz (Fig. 2(c)), the normal dispersion curve is located at Δ_p = -100 MHz or Δ_p = 100 MHz, respectively. When Δ_c = 0 and Δ_s = 100 MHz, these two dispersion curves appear at two different positions Δ_p = 0 and Δ_p = 100 MHz, as shown in Fig. 2(d). For Δ_s = -100 MHz, the second dispersion curve (corresponding to the second EIT window) is shifted to the left and located at the position Δ_p = -100 MHz, as shown in Fig. 2(e). Particularly, for Δ_c = 100 MHz and Δ_s = -100 MHz, two normal dispersion curves are symmetric through the resonance frequency, at the same time in the resonance region is anomalous dispersion, as we see in Fig. 2(f). Thus, the above results show that by changing the frequency of the signal laser field and/or the coupling laser field, the slope, the position, and the shape of dispersion curves are also changed. This can be applied into a two-way conversion between slow light mode and fast light mode as well, which may be developed in future research.

3.2. Controlling width and depth of EIT windows

In this section, our investigations are still conducted at room temperature T = 300 K and the influence of the intensity of the controlling laser fields on EIT spectra of the probe beam is under discussion. Here, the frequency detunings of the controlling laser fields remain constant at Δ_c = 0 and Δ_s =100 MHz while the intensity of the controlling laser fields is varied at different values as: (a) ω_c = 150 MHz and ω_s = 0; (b) ω_c = 0 and ω_s = 150MHz; (c) ω_c = 200 MHz and ω_s = 100 MHz; (d) ω_c = 100 MHz and ω_s = 200 MHz; (e) ω_c = 200 MHz and ω_s = 200 MHz; (f) ω_c = 300 MHz and ω_s = 300 MHz. The variations of the width and depth of the EIT windows according to the controlling laser intensity are plotted as in Fig. 3. Figure 3(a) demonstrates that the absence of the signal laser field (ω_s = 0) results in the excited configuration returning to the basic three-level lambda configuration. This phenomenon also leads to the existence of one EIT window in the absorption spectrum of the probe field at frequency detuning Δ_p = 0. This EIT window consequently appeared due to the action of the coupling laser field (ω_c). The appearance of one EIT window also occurs when the coupling laser field is turned off, as shown in Fig. 3(b). This EIT window is created by the signal laser field with the frequency detuning $\Delta_s = 100$ MHz.

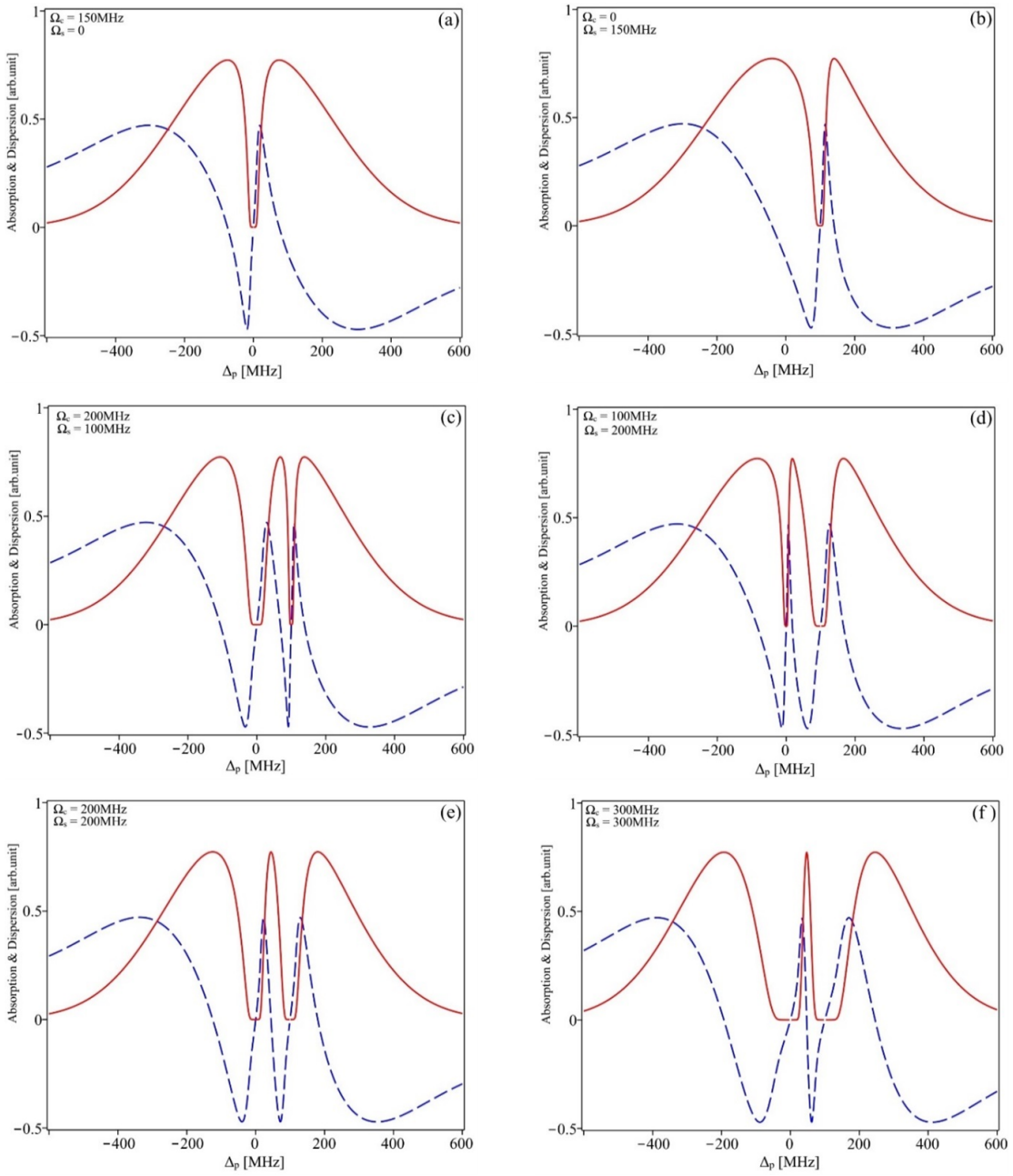

Fig. 3. Absorption and dispersion graphs of the probe laser field at different intensities of the controlling laser fields. The solid lines represent absorption and the dashed lines represent dispersion. The graphs are constructed at a constant temperature 300 K. Other parameters are constant: $\Delta_c = 0$ and Δ_s =100 MHz and $\omega_p = 0.05$ MHz.

With the presence of the two strong controlling laser fields affecting the atomic system, two separated EIT windows appear at the positions $\Delta_p = 0$ and Δ_p =100 MHz. At the intensity of the signal laser field ω_s = 100 MHz and the intensity of the coupling laser field ω_c = 200 MHz, the width of the EIT window at the position $\Delta_p = 0$ is greater than that at the position Δ_p = 100 MHz. Conversely, when the intensity of the two strong controlling laser fields is interchanged (ω_c = 100 MHz and ω_s = 200 MHz) as shown in Fig. 3(d), the width of the EIT windows also changes respectively. These results re-confirm the similar influences of controlling laser fields on the EIT effect in a four-level lambda-type atomic system. In addition, it is easy to see from Fig. 3 that increasing the intensity of the controlling laser fields leads to an increase in the depth of the EIT window. Thus, intensities of controlling laser fields affect the width and depth of EIT windows; in other words, they affect zero-absorption regions of the probe laser field. The application based on that influence may deliver greater opportunities to investigate all optical switching or soliton propagation at EIT windows.

Furthermore, Fig. 3 also illustrates dispersion curves of the medium with respect to the frequency detuning of the probe field when changing the intensity of the controlling laser fields. The change of the width of EIT windows results in the change in the dispersion curves. An increase in intensity of the controlling laser fields reduces the slope of dispersion curves, as shown in Figs. 3(e) and 3(f). This change has a direct effect on group velocity of the probe light, thereby it decides whether the propagation of fast light or slow light occurs.

3.3. The influence of Doppler broadening on double EIT

Finally, we investigate the influence of Doppler broadening on the shape of EIT windows, as depicted in Fig. 4. Here, the intensity of the coupling and signal laser fields remain constant at $\omega_c = \omega_s$ = 100 MHz. The detunings of the two controlling laser fields are selected as $\Delta_c = 0$ and Δ_s =100 MHz for creating two EIT windows at different two positions $\Delta_p = 0$ and Δ_p =100 MHz. The EIT spectra are simulated at different temperatures: (a) T = 10 K, (b) T = 100 K, (c) T = 200 K, (d) T = 300 K, (e) T = 400 K and (f) T = 500 K. From Fig. 4 we can see that at low temperature T = 10 K (Fig. 4(a)), the EIT windows are wide with the great depth and nearly-four-unit height. In addition, the profile of the absorption spectrum is quite small. However, when the temperature increases up to 100 K (Fig. 4(b)), the EIT windows are narrowed and their depth declines down to over one unit. Continuing to increase the temperature up to 200 K (Fig. 4(c)), 300 K (Fig. (d)), 400 K (Fig. 4€), and 500 K (Fig. 4(f)), it is obvious that the depth and width of the EIT windows decrease as the temperature rises. At the same time, the profile of the absorption spectrum is also greatly expanded. The phenomenon can be explained that for the higher temperature, the faster and more chaotic movement of atoms, and hence it reduces quantum inteference and coherence in the atomic system. To clarify the impact of temperature on the EIT profile, we can compare the full-width at half maximum (FWHM) between Figs. 4(a) and 4(f) at temperatures T = 10 K and T = 500 K, respectively. The comparison shows that FWHM in Fig. 4(a) is about 200 MHz, while FWHM in Fig. 4(f) is over 800 MHz. Because FWHM is widened, the double EIT seems to be closer together and the EIT window heights decrease. This leads to the risk of overlapping, thereby causing structural destruction of EIT windows. In other words, EIT efficiency deteriorates sharply at increasing temperature. This is also a reason why studies on EIT in high-temperature media are limited.

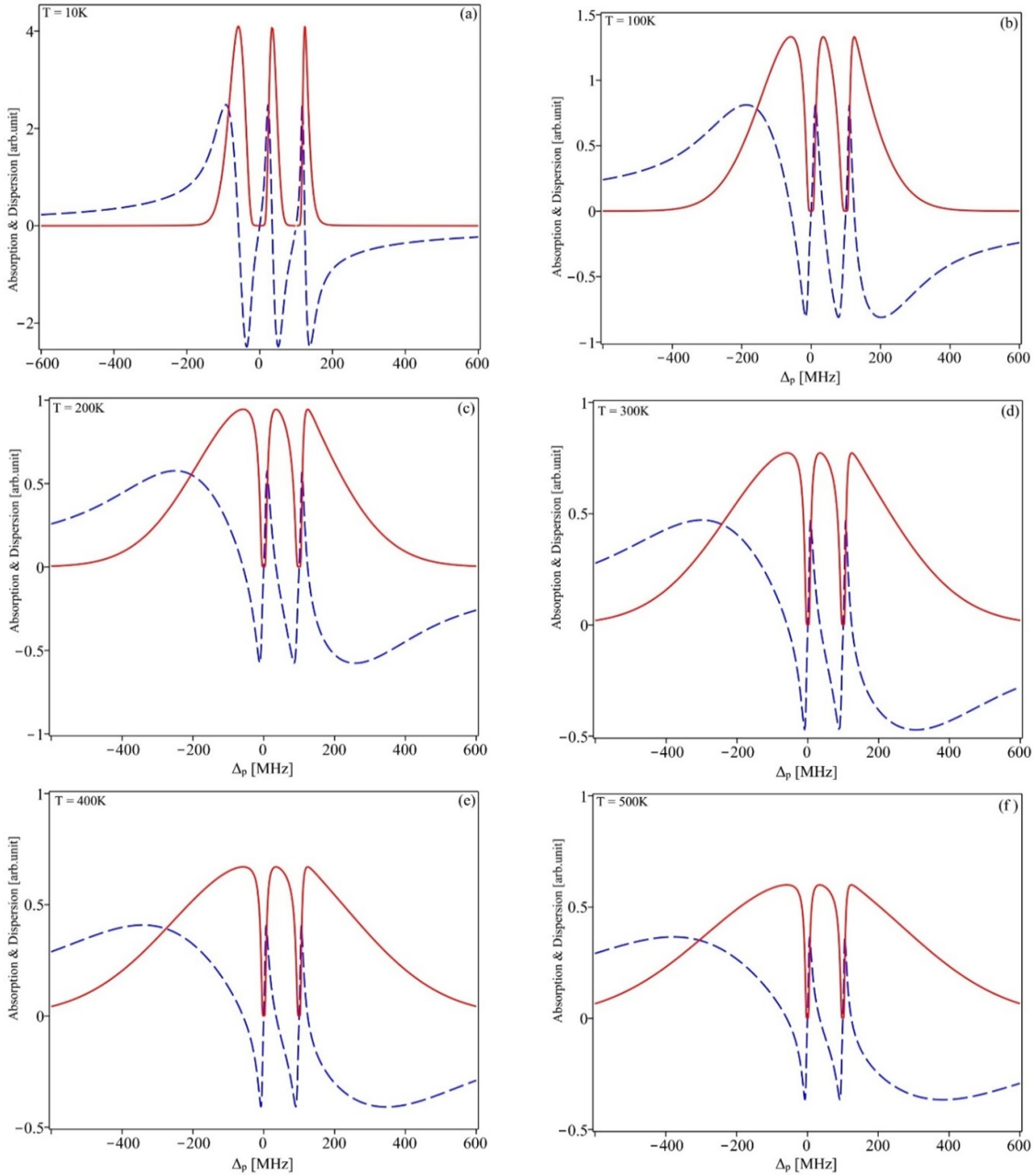

Fig. 4. Absorption and dispersion graphs with respect to the detuning of the probe laser field at different temperatures. The solid lines represent absorption, and the dashed lines represent dispersion. The graphs are constructed with unchanged parameters as follow: $\Delta_c = 0$, Δ_s =100 MHz and $\omega_c = \omega_s$ = 100 MHz.

4. Conclusion

Double electromagnetically induced transparency in the four-level lambda-type atomic system was considered at room temperature with Doppler broadening. Two EIT windows can be created in this system under the induction of coupling or signal fields. The EIT windows can be manipulated independently by the controlling laser fields. The position of the EIT windows are easily shifted by changing the frequency of the controlling laser fields, while the depth and the width of the EIT windows are easily changed by adjusting the intensity of the controlling laser fields. In particular, by turning on or off one of the two controlling laser fields, the probe field response can be switched between one or two EIT window regimes, i.e., it is possible to switch between absorption and transparency regimes, and vice versa. Temperature also has a significant effect on the EIT efficiency; in particular, as the temperature increases, the EIT efficiency decreases, at the same time, the spectral profile is greatly expanded and thus can overlap the EIT windows. Such an analytical model is necessary for experimental observations and related studies at room temperature.

Acknowledgment

This research was funded by Vingroup Innovation Foundation (VINIF) under project code VINIF.2022.DA00076.

References

[1] S. E. Harris, J. E. Field and A. Imamoğlu, *Nonlinear optical processes using electromagnetically induced transparency*, Phys. Rev. Lett. **64** (1990) 1107.
[2] K.-J. Boller, A. Imamoğlu and S. E. Harris, *Observation of electromagnetically induced transparency*, Phys. Rev. Lett. **66** (1991) 2593.
[3] J. Gea-Banacloche, Y.-q. Li, S.-z. Jin and M. Xiao, *Electromagnetically induced transparency in ladder-type inhomogeneously broadened media: Theory and experiment*, Phys. Rev. A **51** (1995) 576.
[4] A. S. Zibrov, C. Y. Ye, Y. V. Rostovtsev, A. B. Matsko and M. O. Scully, *Observation of a three-photon electromagnetically induced transparency in hot atomic vapor*, Phys. Rev. A **65** (2002) 043817.
[5] V. Ahufinger, R. Corbalán, F. Cataliotti, S. Burger, F. Minardi and C. Fort, *Electromagnetically induced transparency in a bose–einstein condensate*, Opt. Commun. **211** (2002) 159.
[6] M. R. N. Surajit Sen, Tushar Kanti Dey and G. Gangopadhyay, *Comparison of electromagnetically induced transparency in lambda, cascade and vee three-level systems*, Journal of Modern Optics **62** (2015) 166 [https://doi.org/10.1080/09500340.2014.960019].
[7] W. Y. X. L. C. D. J. T. Y. He, T. Wang and B. Liu, *All-optical switching based on the electromagnetically induced transparency effect of an active photonic crystal microcavity*, Journal of Modern Optics **61** (2014) 403 [https://doi.org/10.1080/09500340.2014.890251].
[8] H. Li, V. A. Sautenkov, Y. V. Rostovtsev, G. R. Welch, P. R. Hemmer and M. O. Scully, *Electromagnetically induced transparency controlled by a microwave field*, Phys. Rev. A **80** (2009) 023820.
[9] A. Lazoudis, T. Kirova, E. H. Ahmed, P. Qi, J. Huennekens and A. M. Lyyra, *Electromagnetically induced transparency in an open v-type molecular system*, Phys. Rev. A **83** (2011) 063419.
[10] S. R. de Echaniz, A. D. Greentree, A. V. Durrant, D. M. Segal, J. P. Marangos and J. A. Vaccaro, *Observations of a doubly driven v system probed to a fourth level in laser-cooled rubidium*, Phys. Rev. A **64** (2001) 013812.
[11] J. Qi, *Electromagnetically induced transparency in an inverted y-type four-level system*, Physica Scripta **81** (2009) 015402.
[12] H. Li, H. Zhang, H. Sun, X. Hu, D. Sun and X. Li, *Multiple spontaneously generated coherence and phase control of optical bistability and multistability in a tripod four-level atomic medium*, Appl. Opt. **56** (2017) 4995.

[13] D. X. Khoa, N. H. Bang, N. L. T. An, N. V. Phu and L. V. Doai, *An analytical model for cross-kerr nonlinearity in a four-level n-type atomic system with doppler broadening*, Chinese Physics B **31** (2022) 024201.
[14] L. Zhang, Z. Liu and J. Chen, *The electromagnetically induced transparency in the y-type four-level atom system at low light levels*, Science in China Series G: Physics and Astronomy **48** (2005) 593.
[15] N. H. Bang, D. X. Khoa, D. H. Son and L. V. Doai, *Effect of doppler broadening on giant self-kerr nonlinearity in a five-level ladder-type system*, J. Opt. Soc. Am. B **36** (2019) 3151.
[16] D. X. Khoa, P. V. Trong, L. V. Doai and N. H. Bang, *Electromagnetically induced transparency in a five-level cascade system under doppler broadening: an analytical approach*, Physica Scripta **91** (2016) 035401.
[17] Y. Qi, F. Zhou, T. Huang, Y. Niu and S. Gong, *Spatial vector solitons in a four-level tripod-type atomic system*, Phys. Rev. A **84** (2011) 023814.
[18] K. M. Devi, D. R. Chowdhury, G. Kumar and A. K. Sarma, *Dual-band electromagnetically induced transparency effect in a concentrically coupled asymmetric terahertz metamaterial*, Journal of Applied Physics **124** (2018) 063106 [https://pubs.aip.org/aip/jap/article-pdf/doi/10.1063/1.5040734/13894578/063106_1_online.pdf].
[19] B. Bartosz, K. D. Xuan, G. Bogdan, N. S. Vu, Ż. Agnieszka *et al.*, *EIT four-level lambda scheme of cold rubidium atoms*, CMST (2010) 13.
[20] M. O. Scully and M. S. Zubairy, *Quantum Optics, reprint 2001*. 1997.
[21] D. A. Steck, "Rubidium 87 d line data." *Available at http://steck.us/alkalidata*, 2001.